HRI-RECAPP-2015-019; OSU-HEP-15-07

The Diboson Excesses in an Anomaly Free Leptophobic Left-Right Model

Kasinath Das,[1] Tianjun Li,[2,3] S. Nandi,[4] and Santosh Kumar Rai[1]

[1]*Harish-Chandra Research Institute and Regional Centre for Accelerator-based Particle Physics, Chhatnag Road, Jhusi, Allahabad 211019, India*

[2]*State Key Laboratory of Theoretical Physics and Kavli Institute for Theoretical Physics China (KITPC), Institute of Theoretical Physics, Chinese Academy of Sciences, Beijing 100190, P. R. China*

[3]*School of Physical Electronics, University of Electronic Science and Technology of China, Chengdu 610054, P. R. China*

[4]*Department of Physics and Oklahoma Center for High Energy Physics, Oklahoma State University, Stillwater OK 74078-3072, USA*

arXiv:1512.00190v1 [hep-ph] 1 Dec 2015

Abstract

The resonant excesses around 2 TeV reported by the ATLAS Collaboration can be explained in the left-right model, and the tight constraints from lepton plus missing energy searches can be evaded if the $SU(2)_R$ gauge symmetry is leptophobic. We for the first time propose an anomaly free leptophobic left-right model with gauge symmetry $SU(3)_C \times SU(2)_L \times SU(2)_R \times U(1)_X$ where the SM leptons are singlets under $SU(2)_R$. The gauge anomalies are cancelled by introducing extra vector-like quarks. The mass of Z' gauge boson, which cannot be leptophobic, is assumed to be around or above 2.5 TeV so that the constraint on dilepton final state can be avoided. Moreover, we find that the $W' \to WZ$ channel cannot explain the ATLAS diboson excess due to the tension with the constraint on $W' \to jj$ decay mode. We solve this problem by considering the mixings between the SM quarks and vector-like quarks. We show explicitly that the ATLAS diboson excess can be explained in the viable parameter space of our model, which is consistent with all the current experimental constraints.

PACS numbers: 11.10.Kk, 11.25.Mj, 11.25.-w, 12.60.Jv

I. INTRODUCTION

Both the ATLAS and CMS Collaborations have performed searches for the massive resonances decaying into a pair of weak gauge bosons via the jet substructure techniques, *i.e.*, the $pp \to V_1V_2 \to 4j$ ($V_{1,2} = W^\pm$ or Z) channels [1–3]. With 20.3 fb^{-1} of data at 8 TeV LHC beam collision energies, the ATLAS Collaboration have found excesses for narrow width resonances around 2 TeV in the WZ, WW, and ZZ channels with local signal significances of 3.4σ, 2.6σ, and 2.9σ, respectively [1]. Moreover, the CMS Collaboration have done the similar searches, though did not distinguish between W- and Z-tagged jets, uncovering a 1.4σ excess near 1.9 TeV [2]. Interestingly, the CMS Collaboration also reported about 2σ and 2.2σ excesses near 1.8 TeV and 1.8–1.9 TeV in the dijet resonance channel and the $e\nu b\bar{b}$ channel, respectively, which could be explained by a $W' \to Wh$ process [4, 5]. Although they are not yet statistically significant, these anomalous events were interpretated as new physics beyond the Standard Model (SM) due to the correlations among different searches. Recently, these diboson excesses have been extensively studied [6–14, 21–73].

The resonances, which are around 2 TeV and have widths less than about 100 GeV, can address the ATLAS diboson excess. Because such narrow resonances might suggest new weakly interacting particles, we will consider the perturbative theories here. For the ATLAS excesses in the WZ, WW, and ZZ channels, the tagging selections for each mode used in the analyses are rather incomplete, and these channels share about 20% of the events. Thus, it may be difficult to claim that a single resonance is responsible for all excesses, although such possibility exists. The reference ranges of the production cross-section times the decay branching ratio for the 2 TeV resonances in the WZ, WW, and ZZ channels are approximately $4 - 8$ fb, $3 - 7$ fb, and $3 - 9$ fb, respectively. So, we shall consider that the prefered production cross-section times the decay branching is from 5 to 10 fb.

We shall employ the left-right models to explain the ATLAS diboson excess, which have been studied recently by quite a few groups as well (For example, see Refs. [9, 11, 14, 48]). To evade the tight constraints from lepton plus missing energy searches, we shall consider the leptophobic $SU(2)_R$ gauge symmetry. However, in the previous studies of such kind of models, anomaly cancellations have not been considered. In this paper, we for the first time propose an anomaly free leptophobic left-right model with gauge symmetry $SU(3)_C \times SU(2)_L \times SU(2)_R \times U(1)_X$ where the SM leptons are singlets under $SU(2)_R$. To cancel the gauge anomalies, we introduce additional vector-like quarks. Because the Z' gauge boson cannot be leptophobic, we assume its mass to be around or above 2.5 TeV so that the constraint on dilepton final state can be escaped. Moreover, we find that the $W' \to WZ$ channel cannot explain the ATLAS diboson excess due to the tension with the constraint on $W' \to jj$ decay mode. Interestingly, this problem can be solved via the mixings between

the SM quarks and vector-like quarks. We show explicitly that the ATLAS diboson excess can be generated in the viable parameter space of our model, which is consistent with all the current experimental constraints.

This paper is organized as follows. In Section II, we present the anomaly free leptophobic left-right symmetric model. In Section III, we study the ATLAS diboson excess and other phenomenological constraints in details. Our conclusion and summary are given in Section IV.

II. THE ANOMALY FREE LEPTOPHOBIC LEFT-RIGHT SYMMETRIC MODEL

It was observed that in a leptophobic left-right symmetric model, one can indeed explain the diboson excesses within 2σ confidence level [11, 14]. However, in order to escape the constraint from the Z' decay $Z' \to \ell^+\ell^-$, one needs to consider the leptophobic $SU(2)_R$ model. Earlier models along this line have not been free of anomalies. In order to cancel the gauge anomalies, we consider a similar model by introducing extra vector-like quarks in the theory.

In the left-right symmetric model, the gauge symmetry is $SU(3)_C \times SU(2)_L \times SU(2)_R \times U(1)_X$ where $X \equiv B-L$ in the original model [15–20] . We consider that the $SU(2)_R \times U(1)_X$ gauge symmetry is broken down to $U(1)_Y$ by a doublet Higgs field H' around the TeV scale, and the $SU(2)_L \times U(1)_Y$ gauge symmetry is further broken down to $U(1)_{EM}$ via a bidoublet Higgs field Φ and a Higgs doublet H. To cancel the gauge anomalies, we introduce the extra quarks XQ_i^{Rc}, XU_i^c, and XD_i^c, which become vector-like particles after the $SU(2)_R \times U(1)_X$ gauge symmetry breaking. As in the supersymmetric SMs, we denote the SM left-handed quark doublets, right-handed up-type quarks, right-handed down-type quarks, left-handed lepton doublets and right-handed charged leptons as Q_i, U_i^c, D_i^c, L_i and E_i^c, respectively. We also define $Q_i^R \equiv (U_i^c,\ D_i^c)$ and $XQ_i^{Rc} \equiv (XU_i,\ XD_i)$. Thus, $(XU_i,\ XU_i^c)/(XD_i,\ XD_i^c)$ will form the vector-like quarks after the symmetry breaking. We present the particles and their quantum numbers in Table I. It is easy to show that the model is anomaly free. By the way, instead of H', we can also introduce an $SU(2)_R$ triplet Higgs field with $U(1)_X$ charge one to break the $SU(2)_R \times U(1)_X$ gauge symmetry down to $U(1)_{EM}$. However, such triplet Higgs field cannot give the vector-like masses to vector-like particles after gauge symmetry breaking. So we will not consider this kind of scenarios here.

The $SU(2)_R \times U(1)_X$ gauge symmetry is broken down to $U(1)_Y$ via the vacuum expectation value (VEV) of H' as below

$$H' = \begin{pmatrix} \chi'^0 \\ \chi'^- \end{pmatrix} \ , \quad \langle H' \rangle = \frac{1}{\sqrt{2}} \begin{pmatrix} u \\ 0 \end{pmatrix} \ . \tag{1}$$

Q_i	$(\mathbf{3},\mathbf{2},\mathbf{1},\mathbf{1/6})$	Q_i^R	$(\overline{\mathbf{3}},\mathbf{1},\mathbf{2},\mathbf{-1/6})$	$L_i,\ H$	$(\mathbf{1},\mathbf{2},\mathbf{1},\mathbf{-1/2})$
E_i^c	$(\mathbf{1},\mathbf{1},\mathbf{1},\mathbf{1})$	XQ_i^{Rc}	$(\mathbf{3},\mathbf{1},\mathbf{2},\mathbf{1/6})$	XU_i^c	$(\overline{\mathbf{3}},\mathbf{1},\mathbf{1},\mathbf{-2/3})$
XD_i^c	$(\overline{\mathbf{3}},\mathbf{1},\mathbf{1},\mathbf{1/3})$	Φ	$(\mathbf{1},\mathbf{2},\mathbf{2},\mathbf{0})$	H'	$(\mathbf{1},\mathbf{1},\mathbf{2},\mathbf{-1/2})$

TABLE I: The particles and their quantum numbers under the $SU(3)_C \times SU(2)_L \times SU(2)_R \times U(1)_X$ gauge symmetry in Model I.

Subsequently the $SU(2)_L \times U(1)_Y$ gauge symmetry is broken down to $U(1)_{EM}$ via the VEVs of Φ and H as follows

$$H = \begin{pmatrix} \chi^0 \\ \chi^- \end{pmatrix}, \qquad \langle H \rangle = \frac{1}{\sqrt{2}} \begin{pmatrix} v_3 \\ 0 \end{pmatrix},$$
$$\Phi = \begin{pmatrix} \phi_1^0 & \phi_1^+ \\ \phi_2^- & \phi_2^0 \end{pmatrix}, \qquad \langle \Phi \rangle = \frac{1}{\sqrt{2}} \begin{pmatrix} v_1 & 0 \\ 0 & v_2 \end{pmatrix}. \tag{2}$$

As we shall discuss below, H will give masses to the charged leptons. For simplicity, we assume $v_1 >> v_3$ and $v_2 >> v_3$ such that $v = \sqrt{v_1^2 + v_2^2 + v_3^2} \simeq \sqrt{v_1^2 + v_2^2}$. Note that as W' and Z' are around 2-3 TeV, we have $v << u$. So we define a small parameter, $1/x$ where

$$x \ \equiv \ \frac{u^2}{v^2} \ , \tag{3}$$

with $x \gg 1$ and a mixing angle $\beta \equiv \arctan(v_1/v_2)$.

The SM fermion Yukawa terms in both models are

$$-\mathcal{L} = y_{ij}^Q Q_i Q_j^R \Phi \quad + \quad y_{ij}^L L_i E_j^c H \ , \tag{4}$$

where y_{ij}^Q and y_{ij}^L are Yukawa couplings, and $i/j = 1,\ 2,\ 3$. Thus, as in the left-right symmetric models with only one bi-doublet, the SM quark masses and CKM mixings are still a problem, which will be discussed elsewhere.

The additional Yukawa and bilinear mass terms in our model are

$$\begin{aligned} -\mathcal{L} = & \ y_{ij}^{QXU} Q_i X U_j^c \tilde{H} \quad + \quad y_{ij}^{QXD} Q_i X D_j^c H \quad + \quad y_{ij}^{XQU} X Q_i^{Rc} X U_j^c \tilde{H}' \\ & + \ y_{ij}^{XQD} X Q_i^{Rc} X D_j^c H' \quad + \quad \mu_{ij} Q_i^R X Q_j^{Rc} + h.c. \ , \end{aligned} \tag{5}$$

where $\tilde{H} \equiv i\sigma_2 H^*$, $\tilde{H}' \equiv i\sigma_2 H'^*$, y_{ij}^{QXU}, y_{ij}^{QXD}, y_{ij}^{XQU} and y_{ij}^{XQD} are Yukawa couplings, and μ_{ij} are bilinear mass parameters. The y_{ij}^{XQU} and y_{ij}^{XQD} terms will give the masses to the vector-like particles XQ_i^{Rc} and XU_i^c/XD_i^c. Interestingly, after we integrate out the vector-like particles, we have new quark Yukawa terms and they may explain the SM quark masses and CKM mixings, which will be studied elsewhere.

The gauge couplings g_L, g_R, and g_X respectively for $SU(2)_L$, $SU(2)_R$, and $U(1)_X$ are given by

$$g_L = \frac{e}{\sin\theta_W}, \quad g_R = \frac{e}{\cos\theta_W \sin\phi}, \quad g_X = \frac{e}{\cos\theta_W \cos\phi} \ . \tag{6}$$

where e is the $U(1)_{EM}$ gauge coupling, θ_W is the weak mixing angle, and the mixing angle $\phi \equiv \arctan(g_X/g_R)$.

We denote $SU(2)_L \times SU(2)_R \times U(1)_X$ gauge bosons as follows

$$SU(2)_L : \ W^{\pm}_{1,\mu}, \ W^3_{1,\mu} \ ; \quad SU(2)_R : \ W^{\pm}_{2,\mu}, \ W^3_{2,\mu} \ ; \quad U(1)_X : \ X_\mu \ .$$

After gauge symmetry breaking, the mass eigenstates of the charged and neutral gauge bosons at the order of $1/x$ are

$$\begin{aligned}
W^{\pm}_{\mu} &= {W_1}^{\pm}_{\mu} + \frac{\sin\phi \sin 2\beta}{x \tan\theta_W} {W_2}^{\pm}_{\mu} \, , \\
{W'}^{\pm}_{\mu} &= -\frac{\sin\phi \sin 2\beta}{x \tan\theta_W} {W_1}^{\pm}_{\mu} + {W_2}^{\pm}_{\mu} \, , \\
A_\mu &= \sin\theta_W W^3_{1\,\mu} + \cos\theta_W (\sin\phi W^3_{2\,\mu} + \cos\phi X_\mu) \, , \\
Z_\mu &= W^3_{Z\mu} + \frac{\sin\phi \cos^3\phi}{x \sin\theta_W} W^3_{H\mu} \, , \\
Z'_\mu &= -\frac{\sin\phi \cos^3\phi}{x \sin\theta_W} W^3_{Z\mu} + W^3_{H\mu} \, ,
\end{aligned} \tag{7}$$

where W^3_H and W^3_Z are

$$\begin{aligned}
W^3_{H\mu} &= \cos\phi W^3_{2\,\mu} - \sin\phi X_\mu \, , \\
W^3_{Z\mu} &= \cos\theta_W W^3_{1\,\mu} - \sin\theta_W (\sin\phi W^3_{2\,\mu} + \cos\phi X_\mu) \, .
\end{aligned} \tag{8}$$

The corresponding masses for W' and Z' gauge bosons are

$$M^2_{W'^{\pm}} = \frac{e^2 v^2}{4\cos^2\theta_W \sin^2\phi} (x+1) \ , \quad M^2_{Z'} = \frac{e^2 v^2}{4\cos^2\theta_W \sin^2\phi \cos^2\phi} \left(x + \cos^4\phi\right) \ . \tag{9}$$

The relevant Feynman rules of the gauge-fermion couplings for the $SU(2)_L$ doublets (P_L), $SU(2)_R$ doublets (P_R), and $SU(2)_L \times SU(2)_R$ singlets (P_S) are given by

$$W'^{\pm}\overline{f}f' : \quad \frac{e}{\sqrt{2}\sin\theta_W} \left(f_{W'L} P_L + f_{W'R} P_R + f_{W'S} P_S\right) \ , \tag{10}$$

with

$$f_{W'L} = -\frac{\sin\phi \sin(2\beta)}{x \tan\theta_W} \ , \qquad f_{W'R} = \frac{\tan\theta_W}{\sin\phi} \ , \quad f_{W'S} = 0 \ , \tag{11}$$

and

$$Z'\overline{f}f : \quad \frac{e}{\sin\theta_W \cos\theta_W} \left(f_{Z'L} P_L + f_{Z'R} P_R + f_{Z'S} P_S\right) \ , \tag{12}$$

with

$$f_{Z'L} = (T_L^3 - Q)\sin\theta_W \tan\phi - (T_L^3 - Q\sin^2\theta_W)\frac{\sin\phi\cos^3\phi}{x\sin\theta_W} \ , \tag{13}$$

$$f_{Z'R} = (T_R^3 - Q\sin^2\phi)\frac{\sin\theta_W}{\sin\phi\cos\phi} + Q\frac{\sin\theta_W\sin\phi\cos^3\phi}{x} \ , \tag{14}$$

$$f_{Z'S} = -Q\sin\theta_W\tan\phi + Q\frac{\sin\theta_W\sin\phi\cos^3\phi}{x} \ . \tag{15}$$

With all out-going momenta, the gauge boson self-couplings are given as follows. The three-point couplings are

$$V_1^\mu(k_1)V_2^\nu(k_2)V_3^\rho(k_3): \quad -if_{V_1V_2V_3}\left[g^{\mu\nu}(k_1-k_2)^\rho + g^{\nu\rho}(k_2-k_3)^\mu + g^{\rho\mu}(k_3-k_1)^\nu\right] \ , \tag{16}$$

where the coupling strengths $f_{V_1V_2V_3}$ for the WWZ' and $W'WZ$ are

$$f_{WWZ'} = \frac{e\sin\phi\cos^3\phi\cot\theta_W}{x\sin\theta_W} \ , \quad f_{W'WZ} = \frac{e\sin\phi\sin(2\beta)}{x\sin^2\theta_W} \ . \tag{17}$$

We note that the number of physical scalar fields in the model after symmetry breaking is quite large due to the presence of several scalar multiplets [1]. We work in the approximation that of the three remaining CP-even neutral Higgs fields, we assume that we can decouple one of them by appropriate choice of the bare parameters in the scalar potential. Therefore, we assume that only two low-lying CP-even states will have significant mixing. Expanding the Higgs field Φ around the vacuum we have,

$$\Phi = \begin{pmatrix} \frac{v_1+h_1}{\sqrt{2}} & \phi_1^+ \\ \phi_2^- & \frac{v_2+h_2}{\sqrt{2}} \end{pmatrix}.$$

The CP even states would mix and we can write them in terms of the physical basis as

$$\begin{pmatrix} h_1 \\ h_2 \end{pmatrix} = \begin{pmatrix} \cos\alpha & \sin\alpha \\ -\sin\alpha & \cos\alpha \end{pmatrix} \begin{pmatrix} h \\ h' \end{pmatrix} \tag{18}$$

In the decoupling limit where $\alpha = \beta - \frac{\pi}{2}$ we can rewrite the states in terms of the angle defined by the ratio of the two doublet vevs only :

$$\begin{pmatrix} h_1 \\ h_2 \end{pmatrix} = \begin{pmatrix} h\sin\beta - h'\cos\beta \\ h\cos\beta + h'\sin\beta \end{pmatrix} \tag{19}$$

We identify h as the SM Higgs such that the hWW' and hZZ' couplings are given by

$$hWW' : g^{\mu\nu}\frac{e^2v}{2\sin^2\theta_W}f_{HWW'} \ , \quad hZZ' : g^{\mu\nu}\frac{e^2v}{2\sin^2\theta_W\cos^2\theta_W}f_{HZZ'} \ , \tag{20}$$

[1] The details of the full scalar spectrum and its implications will be discussed elsewhere as it would not play a significant role in the explanation of the diboson excess.

where the coupling strengths are

$$f_{hWW'} = -\frac{\sin(2\beta)\tan\theta_W}{\sin\phi} + \frac{\sin(2\beta)(\tan\theta_W - \cot\theta_W \sin^2\phi)}{x\sin\phi} \ , \tag{21}$$

$$f_{hZZ'} = -\frac{\sin\theta_W}{\tan\phi} + \frac{\cos^3\phi(\sin^2\theta_W\cos^2\phi - \sin^2\phi)}{x\sin\theta_W\sin\phi} \ . \tag{22}$$

We now have all the relevant interaction strengths in the model to study the phenomenology of the additional heavy gauge bosons in the theory. In the next section we consider their production at the LHC and how the diboson excess can be explained in our model.

III. THE CONSISTENT DIBOSON EXCESS ANALYSES

The model we propose gives us the heavy gauge bosons $W'^{\pm}$ and Z' with their masses depending on the H' doublet Higgs VEV (u) and $SU(2)_R$ gauge coupling. We note that the diboson excess reported by ATLAS could be the combined contributions from the W' and Z' productions decaying to a pair of electroweak gauge bosons. However, a strong constraint on the dilepton final state suggests that the Z' production with mass of around 2 TeV could be in contradiction to it unless the Z' is leptophobic as well. So we first try and set the parameter space such that the Z' is too heavy and evades such bounds. We shall come back to the Z' phenomenology to see if such a requirement is at all necessary in our model. For simplicity we shall set the mass of Z' to be 2.5 TeV and above. The relevant parameters that need to be considered in the analysis would be the gauge couplings, g_L, g_R and g_X which can be re-parameterised in terms of the known parameters, *viz.* electric charge e, Weinberg angle θ_W, and an additional unknown angle ϕ as shown in Eq. (6). As we would like to achieve a signal for a 2 TeV resonance, the $M_{W'}$ is fixed at that value which in turn makes the ratio $x = u^2/v^2$ dependent on ϕ. Thus, as we change ϕ the VEV u also changes and affects the Z' mass. We plot the dependence of the Z' mass on the value for $\tan\phi$ for a fixed $M_{W'} = 2$ TeV in Fig. 1. As the Z' mass is found to increase with increasing values of $\tan\phi$, the mass of Z′ becomes greater than 2.5 TeV for $\tan\phi$ greater than 0.76.

We also want the 2 TeV resonance to have a narrow width which we achieve by demanding the total decay width Γ of the resonance to satisfy $\Gamma/M_V \leq 0.1$. Since the resonant signal must now come only from the W', we plot the dependence of the width of W′ on $\tan\phi$ in Fig. 2 where again the mass of W' has been set to 2 TeV. It is clear that narrow width approximation is valid for a 2 TeV W' only when $\tan\phi \geq 0.31$.

We now turn our attention to the signal and the parameters that affect the rates, since the on-shell production of the W' depends on the values of ϕ and β. Note that the interaction strengths of the W' to the SM particles suggests that the decay of $W' \to WZ$ can be maximized for $\tan\beta = 1$ while the production of the right-handed gauge boson is enhanced

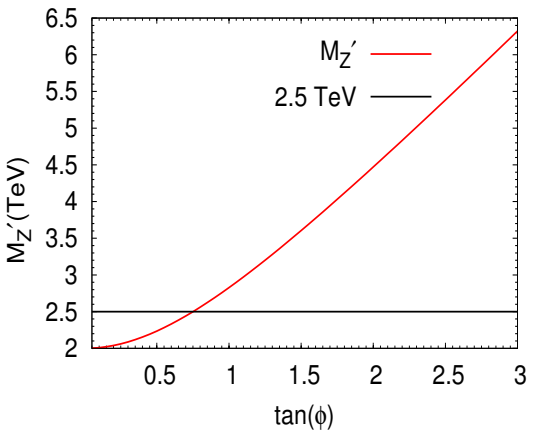

FIG. 1: Mass of Z' versus $\tan\phi$.

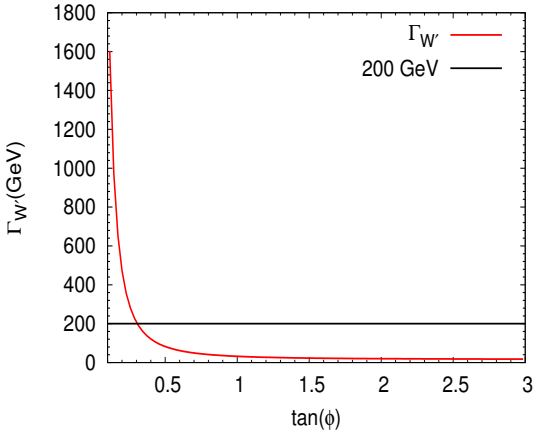

FIG. 2: Width of W′ versus $\tan\phi$.

for smaller values of $\tan\phi$. Therefore, throughout the analysis we have kept $\tan\beta = 1$ and varied $\tan\phi$ as it governs the production of W' as well as its dominant decay channels. We take the range of $\tan\phi$ from 0.75 to 3 to find a viable parameter space in the model which can produce the signal rates for the diboson excess as reported by the ATLAS Collaboration, while satisfying constraints in other channels.

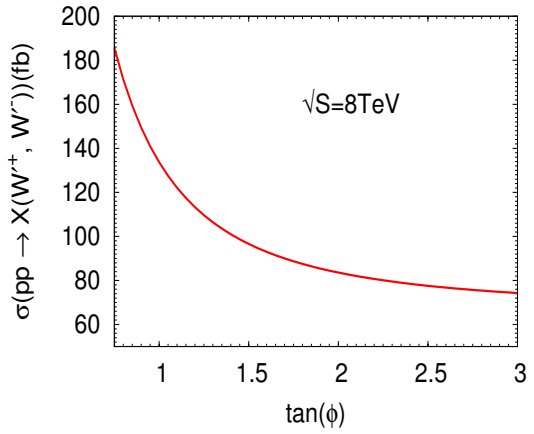

FIG. 3: Production cross section of W' versus $\tan\phi$.

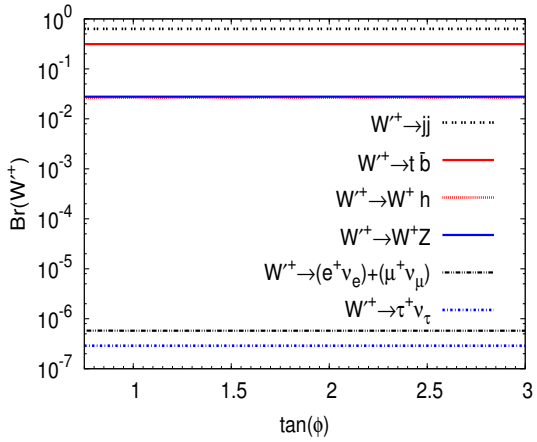

FIG. 4: Branching ratio for different decay channels for W′ versus $\tan\phi$.

In Fig. 3 we plot the production cross section of the W' as a function of $\tan\phi$. The interaction strength of the W' to the quarks become weaker as $\tan\phi$ increases which therefore leads to a drop in the production cross section of the W'. Finally, the final channels observed would depend on how the W' decays and we show this in Fig. 4. As the model by construction makes the W' leptophobic, the branching ratios for W' decaying to leptons and neutrinos are negligible. However, the right-handed gauge boson does have a substantial coupling

strength to the SM quarks and the new exotic heavy quarks which are doublets under the new $SU(2)_R$. This not only helps in producing the W' with large cross sections at the LHC, it also leads to strong signal rates to final states such as jj (sum over first two generations of quarks) and $t\bar{b}$ which are constrained by the LHC data. We choose the heavy exotic vector-like quarks to have mass $M_{XQ} \geq M_{W'}/2$ such that the W' decay to a pair of these exotic quarks is kinematically forbidden. The constraint on the decay mode $W' \to t\bar{b}$ is given by [74]

$$\sigma(pp \to W') \times Br(W' \to t\bar{b}) \lesssim 120 \ fb,$$

while the dijet limits for the jj final state is [75]

$$\sigma(pp \to W') \times Br(W' \to jj) \lesssim 100 \ fb.$$

Another relevant bound is for the $W' \to Wh$ decay mode [4]

$$\sigma(pp \to W') \times Br(W' \to Wh) \lesssim 7 \ fb.$$

From the equivalence theorem for a spontaneously broken gauge symmetry we expect the Wh rates to be around the WZ rate and therefore should satisfy the existing constraints as the signal is expected to be in the same range.

We now analyse and see whether the model can satisfy the constraints and give the required event rates for the diboson excess. To check this we plot the cross section times the branching fractions ($\sigma \times BR$) to different final states in Fig. 5 with the corresponding constraints mentioned in tandem. The horizontal lines with fixed numeric values in the figure represent the respective upper bounds on the final state at the parton level, as presented by the LHC run-I experiment. In the figure we also have illustrated a band with a range of 5-10 fb for the diboson signal which could account for and explain the diboson excess, such that the $\sigma \times BR$ for the $W' \to WZ$ should lie within that band. The dijet and top production rates are found to be still quite large but they do satisfy the existing constraints for nearly the complete range of $\tan\phi$. However, the signal rates for the WZ channel is not adequate to explain the diboson excess. The constraint on $W' \to jj$ decay mode is not satisfied for $\tan\phi$ values below ~ 0.85. However, up till now, we have ignored the fact that there could be significant mixing between the heavy vector-like quarks with the right-handed SM quarks. Such mixings are not very strongly constrained by flavor physics like the left-handed ones. Once allowed, this would not only lead to a suppression in the W' production but will also suppress the decay modes of W' to the quark final states. Such a suppression can lead to an enhancement of the $W' \to WZ$ branching and therefore increase the rates enough to accommodate the diboson excess.

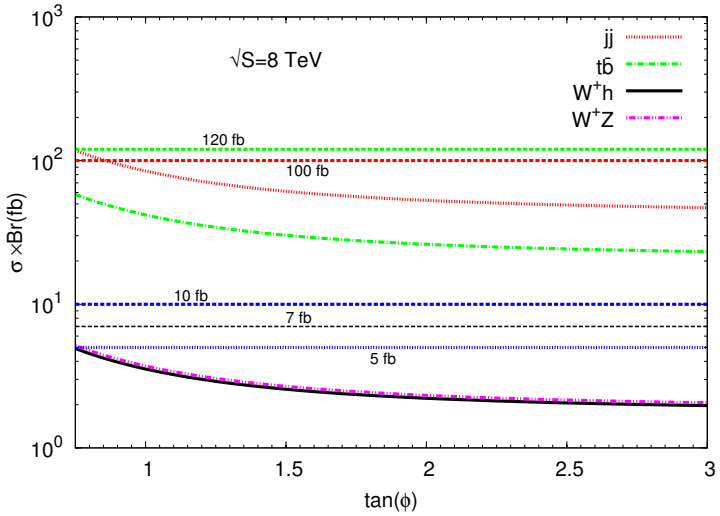

FIG. 5: Cross section times branching ratio for W′ versus $\tan\phi$.

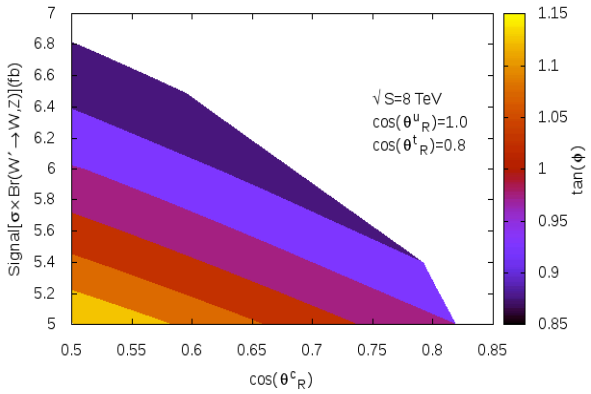

FIG. 6: Signal for cross section times branching ratio for $W' \to WZ$ versus $\cos(\theta_R^c)$ for different values of $\tan\phi$.

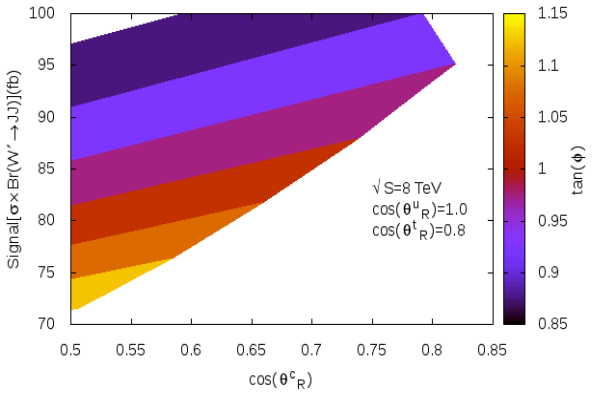

FIG. 7: Signal for cross section times branching ratio for $W' \to jj$ versus $\cos(\theta_R^c)$ for different values of $\tan\phi$.

To achieve $\sigma(pp \to W') \times Br(W' \to WZ) \sim 5 - 10$ fb, we include the following mixing between the right-handed quark and the right-handed new heavy quark sector [2]

$$\begin{pmatrix} u_i' \\ x u_i' \end{pmatrix} = \begin{pmatrix} \cos\theta_R^{u_i} & \sin\theta_R^{u_i} \\ -\sin\theta_R^{u_i} & \cos\theta_R^{u_i} \end{pmatrix} \begin{pmatrix} u_i \\ x u_i \end{pmatrix} \tag{23}$$

[2] We must point out that the masses of the vector-like quarks are required to be similar or above $M_{W'}$ to get an enhancement in the WZ mode. Otherwise, such mixings would lead to new decay modes of W' decaying to a vector-like quark and a SM quark with large branching fractions.

and the resulting doublets are given as

$$Q_i^{R\prime} = \begin{pmatrix} u_i \cos\theta_R^{u_i} + x u_i \sin\theta_R^{u_i} \\ d_i \end{pmatrix}, \qquad XQ_i^{R\prime} = \begin{pmatrix} -u_i \sin\theta_R^{u_i} + x u_i \cos\theta_R^{u_i} \\ x d_i \end{pmatrix} . \tag{24}$$

We do not consider the mixings in the 1st generation quarks which helps in keeping the production cross section for W' unaffected, i.e., we will work with $\cos(\theta_R^u) = 1$. For illustration we choose $\cos(\theta_R^t) = 0.8$ here and vary $0.5 < \cos(\theta_R^c) < 1$. Note that we could equally choose $\cos(\theta_R^t) = 1$ or vary it and we can still get a different but viable range for the parameter space. A similar mixing could also be chosen for the down quark sector which might also help in suppressing contributions to strangeness violating decays. We do not take up this issue here and focus only on the diboson excess. In Fig. 6, we show the allowed parameter space for the mixing angle $\cos(\theta_R^c)$ which gives the desired range of $\sigma(pp \to W') \times Br(W' \to WZ)$ taking values between 5 and 10 fb. Note that the $\tan\phi$ values lie between 0.85 and 1.15. As $\tan\phi$ increases the production cross section falls and therefore the rates decrease as shown in the heat map in Fig. 6 where for $\tan\phi = 1.15$ the diboson rate approaches the lower end of 5 fb. Note that for larger values of $\tan\phi$ one requires smaller $\cos\theta_R^c$ to suppress the dijet branching and increase the WZ branching fraction. Also a slightly larger $\tan\phi$ can be accommodated if both $\cos\theta_R^c$ and $\cos\theta_R^t$ are allowed to vary together. We also show $\sigma(pp \to W') \times Br(W' \to JJ)$ for the allowed parameter region of the scan in Fig. 7. With the run-II of LHC already collecting data at center of mass energy of 13 TeV, a good starting point would be confirm whether any excess observed in the run-I data in various final states or any bumps in invariant mass distributions pointing at physics beyond the SM were not mere fluctuations or misinterpretations of the data. This would also put counter checks on the new physics models that are proposed to explain the aforementioned hints of new, beyond SM physics. To check the validity of our model at the LHC run-II, we estimate the $(\sigma \times Br)$ for WZ and JJ final states for the same range of parameters that could explain the diboson excess observed at run-I. The corresponding results we obtain have been shown in Fig. 8 and Fig. 9 respectively. Quite clearly, the allowed model parameters give a dibson resonance at 2 TeV with a parton cross section for WZ in the range 50-65 fb, while the dijet resonance rate should be less than 950 fb. The above numbers can be easily confirmed to check our model predictions for the observed dibson anomaly at LHC run-II.

We now turn our attention to the other heavy gauge boson (Z') in the theory. Note that we had assumed that the mass of the heavy Z' is above 2.5 TeV and chosen $\tan\phi$ accordingly. As the Z' is an admixture of the $U(1)_X$ and the neutral components of $SU(2)_L$ and $SU(2)_R$ gauge bosons, it cannot be completely leptophobic like the W'. The strong limits on a Z' decaying into the leptonic final states put strong constraints on its mass. Therefore we need to check whether the Z' in our model is indeed required to be much heavier than the W'

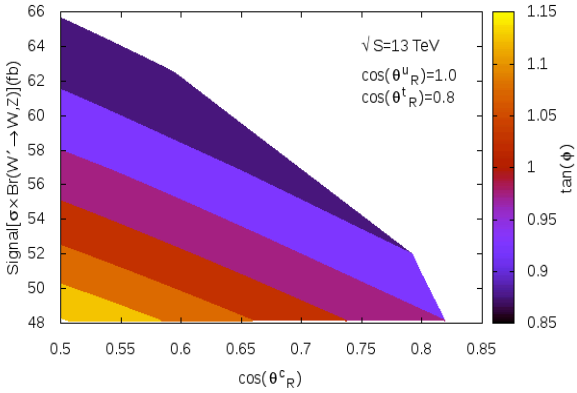

FIG. 8: Signal for cross section times branching ratio for $W' \to WZ$ versus $\cos(\theta_R^c)$ for different values of $\tan\phi$.

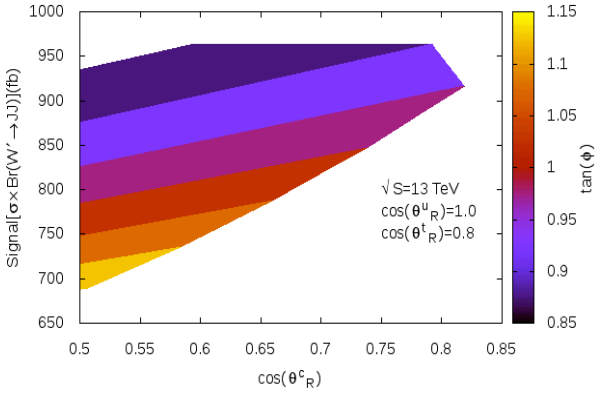

FIG. 9: Signal for cross section times branching ratio for $W' \to jj$ versus $\cos(\theta_R^c)$ for different values of $\tan\phi$.

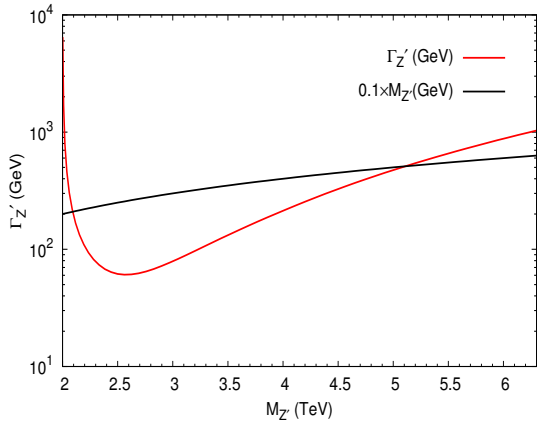

FIG. 10: Width of Z′ versus $M_{Z'}$

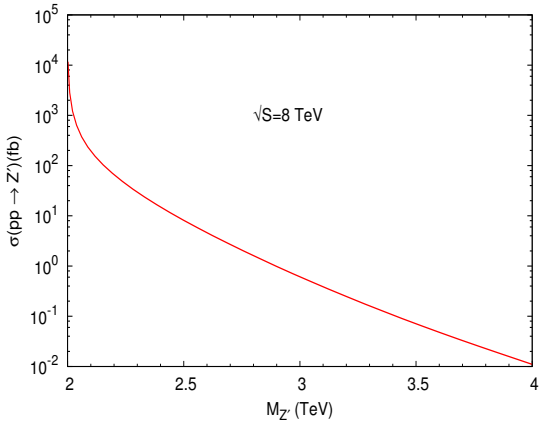

FIG. 11: Production cross section of Z′.

in satisfying all the existing constraints. We do the analysis by keeping $M_{W'} = 2$ TeV. As the Z' mass is dependent on the choice of $\tan\phi$ as shown in Fig. 1, we vary $\tan\phi$ in the range $0.05 - 3$. For this range of $\tan\phi$, $M_{Z'}$ varies from 2 TeV to 6.3 TeV following Eq. (9). However, we have already noted that for W' to have a narrow width, $\tan\phi \geq 0.31$. Thus, the lower choices of $\tan\phi$ are for illustration purposes only and to also highlight the features when the mass is close to the W' mass. As the interactions of Z' with fermions as well as gauge bosons are independent of β (See Eqs. (12)-(22).), the value of $\tan\beta$ does not play a significant role in the Z' phenomenology. Note that the $\tan\phi$ value gives an idea on the width of the W' as well as for the Z'. The value of $\tan\phi$ also determines how large the $SU(2)_R$ and $U(1)_X$ gauge couplings are and therefore would give us the relative

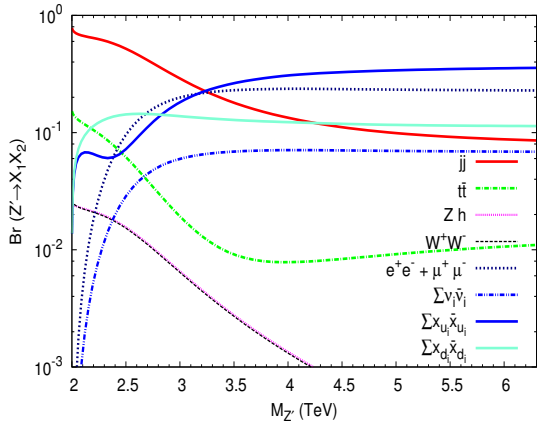

FIG. 12: Branching ratio for different decay modes for Z′ versus $M_{Z'}$.

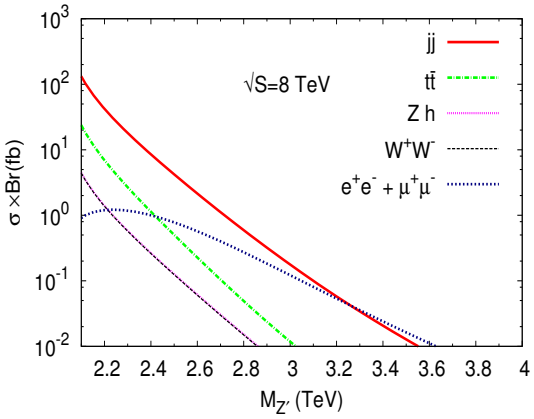

FIG. 13: Cross section times branching ratio for Z′ versus $M_{Z'}$.

characteristics of its leptophobic nature. To obtain the range over which the Z' width is less than $0.1 \times M_{Z'}$ we plot the total width of Z' in Fig. 10 for different values of $M_{Z'}$. It is clear from Fig. 10 that narrow width approximation for Z' is valid for the mass range of 2.1 TeV to 5.1 TeV which implies $\tan\phi$ to be in the range $\sim 0.3 - 2.35$. Note that in the limit $x \gg 1$

$$M_{Z'} \simeq M_{W'}/\cos\phi \ ,$$

which implies that the Z' is always heavier than the W'. Thus, a 2 TeV Z' would lead to a much broader resonance for the W' and itself. We plot the on-shell production cross section of the Z' at LHC with $\sqrt{s} = 8$ TeV in Fig. 11. In the range where the Z' has a small width to ensure narrow width approximation, we can estimate the rates for different final states by multiplying with the corresponding branching fractions. Note that with the narrow width criterion, the $M_{Z'}$ can be as light as 2.1 TeV if it satisfies the current limits set on the different channels. In order to satisfy the diboson excess, the Z' contributions therefore could also contribute to the excess. However, the large production rates for the dijet channel through the W' production could restrict such values for $\tan\phi$. We then might need to include the mixing of the vector-like quarks with the first generation quarks to suppress the dijet rates.

To check the signal strength for different channels we have calculated the branching fractions of the Z' decay which we show in Fig. 12. As the interaction strength of Z' to leptons increases with $\tan\phi$ (see Eqs. (12)-(15)), this leads to the increase in branching ratio for Z' decaying to leptons. This is because the $U(1)_X$ gauge coupling becomes larger for larger values of $\tan\phi$ thus making the Z' less leptophobic. However with increasing $\tan\phi$ the Z' mass also increases and therefore the dilepton channel will not be strongly constrained for such a heavy Z' by the run-I data at LHC. In Fig. 13 we have plotted $(\sigma \times BR)$ for

different final states. The upper limit for dijet resonance given in the CMS dijet analysis [75] is satisfied for $M_{Z'} > 2.3$ TeV. However, allowing mixing between the vector-like quarks with the SM quarks will again dilute the dijet rates and allow a slightly lighter Z'. This mixing would further increase the branching fraction of the Z' decaying leptonically and therefore beyond $M_{Z'} > 2.4$ TeV, it would provide the best mode of discovery at the current run-II of LHC [3]. In addition we find that a dominant mode of decay for the Z' is to a pair of vector-like quarks. Now, the exact rates would depend on the mass of these exotic quarks as well as the mixings they posess with SM like quarks. But the most interesting aspect would be the resonant production of such colored exotics through a Z' leading to enhanced production rates for a pair as well as single production modes (when mixing with SM quarks is subtantial) which could give new signals at the run-II of LHC and its future runs.

IV. CONCLUSION

We employed the left-right models to explain the ATLAS diboson excess. To escape the tight constraints from lepton plus missing energy searches, we required the $SU(2)_R$ gauge symmetry to be leptophobic. However, in the previously considered models, anomaly cancellations have not been ensured. Therefore, we for the first time propose an anomaly free leptophobic left-right model with gauge symmetry $SU(3)_C \times SU(2)_L \times SU(2)_R \times U(1)_X$, where the SM leptons are singlets under $SU(2)_R$. To cancel the gauge anomalies, we introduced the extra vector-like quarks. Since the Z' gauge boson cannot be leptophobic, we assume its mass to be around or above 2.5 TeV and then the constraint on dilepton final state can be avoided. In addition, we found that the $W' \to WZ$ channel cannot explain the ATLAS diboson excess if we included the constraint on $W' \to jj$ decay mode. Interestingly, we solved this problem by considering the mixings between the SM quarks and vector-like quarks. We showed explicitly that the ATLAS diboson excess can be explained in the viable parameter space of our model, which is consistent with all the current experimental constraints. In addition, we have also given predictions for the dijet and WZ channel at the current run of LHC with $\sqrt{s} = 13$ TeV and discussed the ensuing phenomenology of Z' for the viable parameter space of our model. We also propose new signals for the vector-like quarks in our model which can be studied at the high energy run of the LHC.

[3] With the increase in leptonic branching for a heavier Z', one can in principle accommodate the 2.9 TeV anomalous resonant event reported in the early data of run-II by CMS in the leptonic final state [76] in our model.

ACKNOWLEDGMENTS

This research was supported in part by the Department of Atomic Energy, Government of India, for the Regional Centre for Accelerator-based Particle Physics (RECAPP), Harish-Chandra Research Institute (KD, SKR), by the Natural Science Foundation of China under grant numbers 11135003, 11275246, and 11475238 (TL) and by the US Department of Energy Grant Number DE-SC0010108 (SN).

---

[1] G. Aad *et al.* [ATLAS Collaboration], arXiv:1506.00962 [hep-ex].

[2] V. Khachatryan *et al.* [CMS Collaboration], JHEP **1408**, 173 (2014) [arXiv:1405.1994 [hep-ex]].

[3] V. Khachatryan *et al.* [CMS Collaboration], JHEP **1408**, 174 (2014) [arXiv:1405.3447 [hep-ex]].

[4] V. Khachatryan *et al.* [CMS Collaboration], arXiv:1506.01443 [hep-ex].

[5] The CMS Collaboration, note PAS-EXO-14-010, March 2015.

[6] H. S. Fukano, M. Kurachi, S. Matsuzaki, K. Terashi and K. Yamawaki, arXiv:1506.03751 [hep-ph].

[7] J. Hisano, N. Nagata and Y. Omura, arXiv:1506.03931 [hep-ph].

[8] K. Cheung, W. Y. Keung, P. Y. Tseng and T. C. Yuan, arXiv:1506.06064 [hep-ph].

[9] B. A. Dobrescu and Z. Liu, arXiv:1506.06736 [hep-ph].

[10] A. Alves, A. Berlin, S. Profumo and F. S. Queiroz, arXiv:1506.06767 [hep-ph].

[11] Y. Gao, T. Ghosh, K. Sinha and J. H. Yu, arXiv:1506.07511 [hep-ph].

[12] A. Thamm, R. Torre and A. Wulzer, arXiv:1506.08688 [hep-ph].

[13] J. Brehmer, J. Hewett, J. Kopp, T. Rizzo and J. Tattersall, arXiv:1507.00013 [hep-ph].

[14] Q. H. Cao, B. Yan and D. M. Zhang, arXiv:1507.00268 [hep-ph].

[15] J. C. Pati and A. Salam, Phys. Rev. D **10** (1974) 275.

[16] R. N. Mohapatra and J. C. Pati, Phys. Rev. D **11** (1975) 2558.

[17] G. Senjanović and R. N. Mohapatra, Phys. Rev. D **12** (1975) 1502.

[18] G. Senjanović, Nucl. Phys. B **153** (1979) 334.

[19] R. N. Mohapatra and G. Senjanović, Phys. Rev. Lett. **44**, 912 (1980).

[20] R. N. Mohapatra and G. Senjanović, Phys. Rev. D **23**, 165 (1981).

[21] G. Cacciapaglia and M. T. Frandsen, arXiv:1507.00900 [hep-ph].

[22] T. Abe, R. Nagai, S. Okawa and M. Tanabashi, arXiv:1507.01185 [hep-ph].

[23] B. C. Allanach, B. Gripaios and D. Sutherland, arXiv:1507.01638 [hep-ph].

[24] T. Abe, T. Kitahara and M. M. Nojiri, arXiv:1507.01681 [hep-ph].

[25] A. Carmona, A. Delgado, M. Quiros and J. Santiago, arXiv:1507.01914 [hep-ph].

[26] C. W. Chiang, H. Fukuda, K. Harigaya, M. Ibe and T. T. Yanagida, arXiv:1507.02483 [hep-ph].

[27] G. Cacciapaglia, A. Deandrea and M. Hashimoto, arXiv:1507.03098 [hep-ph].

[28] H. S. Fukano, S. Matsuzaki and K. Yamawaki, arXiv:1507.03428 [hep-ph].

[29] V. Sanz, arXiv:1507.03553 [hep-ph].

[30] C. H. Chen and T. Nomura, Phys. Lett. B **749**, 464 (2015) [arXiv:1507.04431 [hep-ph]].

[31] Y. Omura, K. Tobe and K. Tsumura, arXiv:1507.05028 [hep-ph].

[32] L. A. Anchordoqui, I. Antoniadis, H. Goldberg, X. Huang, D. Lust and T. R. Taylor, Phys. Lett. B **749**, 484 (2015) [arXiv:1507.05299 [hep-ph]].

[33] W. Chao, arXiv:1507.05310 [hep-ph].

[34] L. Bian, D. Liu and J. Shu, arXiv:1507.06018 [hep-ph].

[35] D. Kim, K. Kong, H. M. Lee and S. C. Park, arXiv:1507.06312 [hep-ph].

[36] K. Lane and L. Prichett, arXiv:1507.07102 [hep-ph].

[37] A. E. Faraggi and M. Guzzi, arXiv:1507.07406 [hep-ph].

[38] M. Low, A. Tesi and L. T. Wang, arXiv:1507.07557 [hep-ph].

[39] S. P. Liew and S. Shirai, arXiv:1507.08273 [hep-ph].

[40] H. Terazawa and M. Yasue, arXiv:1508.00172 [hep-ph].

[41] P. Arnan, D. Espriu and F. Mescia, arXiv:1508.00174 [hep-ph].

[42] C. Niehoff, P. Stangl and D. M. Straub, arXiv:1508.00569 [hep-ph].

[43] S. Fichet and G. von Gersdorff, arXiv:1508.04814 [hep-ph].

[44] C. Petersson and R. Torre, arXiv:1508.05632 [hep-ph].

[45] F. F. Deppisch, L. Graf, S. Kulkarni, S. Patra, W. Rodejohann, N. Sahu and U. Sarkar, arXiv:1508.05940 [hep-ph].

[46] J. A. Aguilar-Saavedra, JHEP **1510**, 099 (2015) [arXiv:1506.06739 [hep-ph]].

[47] L. Bian, D. Liu, J. Shu and Y. Zhang, arXiv:1509.02787 [hep-ph].

[48] P. S. Bhupal Dev and R. N. Mohapatra, Phys. Rev. Lett. **115**, no. 18, 181803 (2015) [arXiv:1508.02277 [hep-ph]].

[49] D. B. Franzosi, M. T. Frandsen and F. Sannino, arXiv:1506.04392 [hep-ph].

[50] T. Li, J. A. Maxin, V. E. Mayes and D. V. Nanopoulos, arXiv:1509.06821 [hep-ph].

[51] H. Fritzsch, arXiv:1507.06499 [hep-ph].

[52] A. Dobado, F. K. Guo and F. J. Llanes-Estrada, arXiv:1508.03544 [hep-ph].

[53] S. Zheng, arXiv:1508.06014 [hep-ph].

[54] F. J. Llanes-Estrada, A. Dobado and R. L. Delgado, arXiv:1509.00441 [hep-ph].

[55] C. H. Chen and T. Nomura, arXiv:1509.02039 [hep-ph].

[56] U. Aydemir, D. Minic, C. Sun and T. Takeuchi, arXiv:1509.01606 [hep-ph].

[57] T. Bandyopadhyay, B. Brahmachari and A. Raychaudhuri, arXiv:1509.03232 [hep-ph].

[58] A. Dobado, R. L. Delgado and F. J. Llanes-Estrada, arXiv:1509.04725 [hep-ph].

[59] B. A. Arbuzov and I. V. Zaitsev, arXiv:1510.02312 [hep-ph].

[60] D. Aristizabal Sierra, J. Herrero-Garcia, D. Restrepo and A. Vicente, arXiv:1510.03437 [hep-ph].

[61] A. Dobado, R. L. Delgado, F. J. Llanes-Estrada and D. Espriu, arXiv:1510.03761 [hep-ph].

[62] P. Ko and T. Nomura, arXiv:1510.07872 [hep-ph].

[63] J. H. Collins and W. H. Ng, arXiv:1510.08083 [hep-ph].

[64] B. C. Allanach, P. S. B. Dev and K. Sakurai, arXiv:1511.01483 [hep-ph].

[65] B. A. Dobrescu and P. J. Fox, arXiv:1511.02148 [hep-ph].

[66] B. Bhattacherjee, P. Byakti, C. K. Khosa, J. Lahiri and G. Mendiratta, arXiv:1511.02797 [hep-ph].

[67] A. Sajjad, arXiv:1511.02244 [hep-ph].

[68] Z. W. Wang, F. S. Sage, T. G. Steele and R. B. Mann, arXiv:1511.02531 [hep-ph].

[69] A. Alves, D. A. Camargo and A. G. Dias, arXiv:1511.04449 [hep-ph].

[70] T. Appelquist, Y. Bai, J. Ingoldby and M. Piai, arXiv:1511.05473 [hep-ph].

[71] B. Allanach, F. S. Queiroz, A. Strumia and S. Sun, arXiv:1511.07447 [hep-ph].

[72] Q. H. Cao, B. Yan and D. M. Zhang, Phys. Rev. D **92**, no. 9, 095025 (2015). doi:10.1103/PhysRevD.92.095025

[73] W. Z. Feng, Z. Liu and P. Nath, arXiv:1511.08921 [hep-ph].

[74] G. Aad *et al.* [ATLAS Collaboration], Phys. Lett. B **743**, 235 (2015) doi:10.1016/j.physletb.2015.02.051 [arXiv:1410.4103 [hep-ex]].

[75] V. Khachatryan *et al.* [CMS Collaboration], Phys. Rev. D **91**, no. 5, 052009 (2015) doi:10.1103/PhysRevD.91.052009 [arXiv:1501.04198 [hep-ex]].

[76] The CMS Collaboration, "Event display of a candidate electron-positron pair with an invariant mass of 2.9 TeV", note CMS-DP-2015-039, August 2015.